

Preparation of LiTi_2O_4 as a Lithium-ion Battery Anode by a Carbon-thermal Reduction Method

Jiang Zhao^{1, 2, *}, Qingling Shi¹, Yangjun Xiang¹, Yuanyuan Xia¹

¹Jiangsu Provincial Engineering Laboratory for RF Integration and Micropackaging, College of Electronic Science and Engineering, Nanjing University of Posts and Telecommunications, Nanjing 210023, P. R. China

²School of Chemistry & Chemical Engineering, Nanjing University, Nanjing 210023, P. R. China

*E-mail: jzhao_njupt@126.com

Received: 27 June 2017 / Accepted: 7 November 2017 / Published: 28 December 2017

The anode material LiTi_2O_4 was successfully synthesized by a carbon-thermal reduction method. The standard Gibbs free energy of formation of LiTi_2O_4 is estimated by bond enthalpy, and the thermodynamics of the carbon-thermal reaction are calculated. The microstructure of the LiTi_2O_4 sample is obtained by scanning electron microscope (SEM) and X-ray diffraction (XRD). The results show that the as-prepared LiTi_2O_4 has a spinel structure (space group $Fd3m$) and that the average particle size is approximately 0.4-1.2 μm . LiTi_2O_4 shows excellent electrochemical performance in terms of galvanostatic charge/discharge tests, specific capacity and cycling performance. Electrochemical measurements indicate that the symmetrical redox peaks are observed at approximately 1.52 V, and the reversible capacity is approximately 135.9 mAh/g at a rate of 0.2 C.

Keywords: Thermodynamics calculation; LiTi_2O_4 ; Carbon-thermal reduction; Lithium-ion battery

1. INTRODUCTION

Since their first commercialization by Sony Corporation in 1991, lithium-ion batteries have been widely utilized in various electronic devices, such as mobile phones, notebook computers, electric vehicles, and renewable energy storage systems [1-5]. Currently, commercially available lithium-ion batteries predominately use graphite as the anode material. However, they suffer from serious safety problems, which have hampered their further development [6, 7]. To replace conventional carbon-based anodes, several studies have focused on exploiting novel anode materials. Among the candidates for new anode materials, spinel-type lithium titanate, $\text{Li}_{1+x}\text{Ti}_{2-x}\text{O}_4$ ($0 \leq x \leq 1/3$), with a wide composition range, has attracted considerable attention because of its intrinsic

characteristics. For $x=1/3$ at one end, $\text{Li}_{1+1/3}\text{Ti}_{2-1/3}\text{O}_4$ ($\text{Li}_4\text{Ti}_5\text{O}_{12}$) has been the most studied and interesting candidate in negative electrodes because of several inherent advantages [8]. $\text{Li}_4\text{Ti}_5\text{O}_{12}$ has a significant flat charge and discharge plateau, at approximately 1.55 V versus Li/Li^+ , and exhibits zero volume change during lithiation, in which it avoids the SEI formation [7, 9, 10]. However, it is worth noting that the electric conductivity of $\text{Li}_4\text{Ti}_5\text{O}_{12}$ is only approximately 10^{-9} S/cm at 20 °C, resulting in poor rate capability of the batteries [11]. For the other end ($x=0$), LiTi_2O_4 has a spinel crystal structure with the $Fd3m$ space group and cubic symmetry, being expressed as AB_2O_4 with an anion sub lattice of face-centred-cubic closed packing, in which $8a$ tetrahedral sites are located by lithium ions, $16d$ octahedral sites are located by titanium ions, and $32e$ sites are located by oxide ions [12]. Moreover, LiTi_2O_4 is superconductor with $T_c=11$ K, which was first discovered by Johnston in 1973 [13]. However, as the anode, LiTi_2O_4 receives less attention, although its electronic conductivity is higher than $\text{Li}_4\text{Ti}_5\text{O}_{12}$ [14]. It is difficult to fabricate pure phase LiTi_2O_4 because lithium ions in the compounds are easily evaporated and the titanium (III) is easy to oxidize during the synthesis reaction [15]. To date, several methods have been proposed for synthesizing LiTi_2O_4 . For example, a conventional solid-state reaction was employed for the preparation of a LiTi_2O_4 powder sample using LiOH , TiO_2 and Ti_2O_3 (or Ti) in an inert atmosphere at 750 ~ 890 °C [14, 15]. Jiang accurately controlled the stoichiometry and prepared spinel-type LiTi_2O_4 by electrochemical insertion of lithium ions into solid anatase-type TiO_2 in molten LiCl [16]. Kumatani and Jin reported that high quality epitaxial LiTi_2O_4 thin films could be successfully grown by pulsed laser deposition (PLD) [17, 18]. These preparation processes are always complicated and uneconomical.

In this paper, we report a carbon-thermal reduction process for the fabrication of LiTi_2O_4 material using Li_2CO_3 , TiO_2 and a slight excess of starch. To confirm the feasibility of carbon-thermal reduction, the thermodynamics of the reaction process are estimated through the standard Gibbs free energy of formation for LiTi_2O_4 , estimated by bond enthalpy. The microstructure and electrochemical performances of the as-prepared LiTi_2O_4 have been discussed.

2. EXPERIMENTAL

2.1 Synthesis of LiTi_2O_4

The LiTi_2O_4 anode material was synthesized by the carbon-thermal reduction method, using Li_2CO_3 , TiO_2 and 10% (mass fraction) excess starch. Starch (carbon source) was carbonized under high temperature. In brief, some percentage of the starting materials were put into the agate mortar and ground in ethanol by wet milling for 1 h, followed by drying the mixture at 80 °C. Finally, the powders were sintered at 900 °C for 48 h under a dry argon atmosphere to obtain highly crystallized LiTi_2O_4 .

2.2 Structure characterization and electrochemical evaluation

The surface morphology of as-prepared LiTi_2O_4 was determined using a field emission scanning electron microscope (Ultra 55, Carl Zeiss). The crystal structure of the obtained sample was

characterized by X-ray diffraction (XRD) using a Netherlands X' Pert PRO diffractometer and Cu K α radiation.

The electrochemical characterizations were performed using a two-electrode electrochemical cell. For the fabrication of the working electrode, a slurry consisting of 80 wt.% LiTi₂O₄ powders (active material), 10 wt.% acetylene black (electronic conductor), and 10 wt.% polyvinylidene fluoride (PVDF) dissolved in *N*-methyl-2-pyrrolidone (NMP) (binder) was spread uniformly on an aluminium foil current collector. The electrode was dried at 80 °C for 12 h in a vacuum. The test cells were assembled in an argon-filled glove box. The metallic lithium foil was used for the counter electrode, and the two electrodes were separated by a porous polypropylene film (Celgard 2300). LiPF₆ (1 mol·L⁻¹), in a mixture of ethylene carbonate (EC), dimethyl carbonate (DMC) and diethyl carbonate (DEC) (2:2:1 weight ratio), was used as the electrolyte. Cyclic voltammetry (CV) experiments were performed by an electrochemical workstation (CHI 660 D) with a scale rate of 0.5 mV·s⁻¹ at room temperature. Charge/discharge cycling experiments were carried out using a Neware Charge–discharge device (Shenzhen Neware Corporation, China) in the range of 1.0~3.2 V vs. Li/Li⁺ at room temperature.

3. RESULTS AND DISCUSSION

3.1 Thermodynamic analysis

The carbon-thermal reduction method is widely used in metallurgy, resulting from carbon acting as an ample reducing agent; its principle can be expressed as the following equations:



where M is short for metal. When the temperature is high, a strong reducing atmosphere produced from reaction (2) results in the reduction of most metallic oxides. The reduction difficulty is determined by the standard Gibbs free energy of formation of the metal oxides.

A solid phase reaction must follow the principle of thermodynamics, that is, the change of Gibbs free energy for the whole reaction is less than zero. At present, the related thermodynamic data of LiTi₂O₄ are unavailable from physicochemical handbooks or literature, and there is no phase diagram of the Li-Ti-O system for guidance. Bond enthalpy, however, can be used to estimate the standard Gibbs free energy of formation ($\Delta_f G^\ominus$) of some unknown compounds.

Here, we estimated the standard Gibbs free energy of formation of LiTi₂O₄ by bond enthalpy and calculated the thermodynamics for the formation of LiTi₂O₄ using the carbon-thermal reaction method. According to Pauling's quantum theory of chemical bonding and assuming that a molecular total enthalpy is the sum of each individual bond enthalpy, the standard formation enthalpy of the compound ($\Delta_f H_{298}^\ominus$) can be calculated by the enthalpy change of atoms (gas) combined into gaseous compounds. Therefore, the standard enthalpy change (ΔH_0^\ominus) of each monatomic gas needs to be calculated.

The component of LiTi_2O_4 can be assumed to be $\frac{1}{2}\text{Li}_2\text{O} \cdot \text{TiO}_2 \cdot \frac{1}{2}\text{Ti}_2\text{O}_3$, and the chemical bonding can be approximated as $\frac{1}{2}(\text{Li}-\text{O}-\text{Li}) \cdot (\text{O}=\text{Ti}=\text{O}) \cdot \frac{1}{2}(\text{O}=\text{Ti}-\text{O}-\text{Ti}=\text{O})$. Therefore, it can be considered that LiTi_2O_4 contains approximately one Li-O bond and seven Ti-O bonds. From the Handbook of Chemistry and Physics, the bond enthalpy of a Li-O bond is approximately $340.60 \text{ kJ}\cdot\text{mol}^{-1}$, and the bond enthalpy of a Ti-O bond is approximately $661.90 \text{ kJ}\cdot\text{mol}^{-1}$. Assuming that $\text{Li}(\text{g}) + 2\text{Ti}(\text{g}) + 4\text{O}(\text{g}) = \text{LiTi}_2\text{O}_4(\text{g})$, the total bond enthalpy of $\text{LiTi}_2\text{O}_4(\text{g})$ is calculated as

$$\Delta H = -(1 \times 340.60 + 7 \times 661.90) \text{ kJ}\cdot\text{mol}^{-1} = -4973.90 \text{ kJ}\cdot\text{mol}^{-1}.$$

The standard enthalpy change (ΔH_{298}^\ominus) of each gaseous atom can be expressed as

$$\text{Li}(\text{s}) = \text{Li}(\text{g}) \quad \Delta H_{298}^\ominus = 159.30 \text{ kJ}\cdot\text{mol}^{-1}$$

$$\text{Ti}(\text{s}) = \text{Ti}(\text{g}) \quad \Delta H_{298}^\ominus = 473.63 \text{ kJ}\cdot\text{mol}^{-1}$$

$$\frac{1}{2} \text{O}_2(\text{g}) = \text{O}(\text{g}) \quad \Delta H_{298}^\ominus = 249.17 \text{ kJ}\cdot\text{mol}^{-1}$$

Therefore, it can be calculated that $\Delta H_0 = \sum \Delta H_{298}^\ominus = (1 \times 159.30 + 2 \times 473.63 + 4 \times 249.17) \text{ kJ}\cdot\text{mol}^{-1} = 2103.25 \text{ kJ}\cdot\text{mol}^{-1}$.

The standard enthalpy change of LiTi_2O_4 can be calculated as $\Delta_f H_{298, \text{LiTi}_2\text{O}_4}^\ominus = \Delta H + \Delta H_0 = (-4973.90 + 2103.25) \text{ kJ}\cdot\text{mol}^{-1} = -2870.65 \text{ kJ}\cdot\text{mol}^{-1}$.

Next, a semi-empirical equation is used to approximately derivate the standard formation entropy of LiTi_2O_4 ($\Delta_f S_{298}^\ominus$). The semi-empirical equation is represented as shown below:

$$\Delta_f S_{298}^\ominus = \frac{3}{2} R \ln Ar_i - 1.5 \frac{Z_i^2}{r_i} \quad (5)$$

where R is the gas constant ($\text{J}\cdot\text{mol}^{-1}\cdot\text{K}^{-1}$), Ar_i is the relative atomic mass of i element, Z_i is the valence number of i ion, and r_i is the radius of i ion (10^{-10} m).

From the periodic table and the Handbook of Physics and Chemistry, each parameter is obtained as follows:

$$Ar_{\text{Li}} = 6.9, \quad Z_{\text{Li}^+} = 1, \quad r_{\text{Li}^+} = 0.68 \times 10^{-10} \text{ m}, \quad Ar_{\text{Ti}} = 47.9, \quad Z_{\text{Ti}^{3.5+}} = 3.5, \\ r_{\text{Ti}^{3.5+}} = \frac{r_{\text{Ti}^{3+}} + r_{\text{Ti}^{4+}}}{2} = \frac{0.77 \times 10^{-10} + 0.68 \times 10^{-10}}{2} \text{ m} = 0.725 \times 10^{-10} \text{ m}, \quad Ar_{\text{O}} = 16.0, \quad Z_{\text{O}^{2-}} = 2, \quad \text{and} \\ r_{\text{O}^{2-}} = 1.40 \times 10^{-10} \text{ m}.$$

The above data are substituted into formula (5) to get

$$S_{298, \text{Li}^+}^\ominus = 21.88 \text{ J}\cdot\text{mol}^{-1}\cdot\text{K}^{-1},$$

$$S_{298, \text{Ti}^{3.5+}}^\ominus = 22.91 \text{ J}\cdot\text{mol}^{-1}\cdot\text{K}^{-1},$$

$$S_{298, \text{O}^{2-}}^\ominus = 30.29 \text{ J}\cdot\text{mol}^{-1}\cdot\text{K}^{-1}.$$

From the reaction equation, $\text{Li}(\text{s}) + 2\text{Ti}(\text{s}) + 4 \cdot \frac{1}{2} \text{O}_2(\text{g}) = \text{LiTi}_2\text{O}_4(\text{s})$, the standard formation of entropy of LiTi_2O_4 ($\Delta_f S_{298}^\ominus$) can be obtained as follows:

$$\Delta_f S_{298, \text{LiTi}_2\text{O}_4}^\ominus = S_{298, \text{LiTi}_2\text{O}_4}^\ominus - S_{298, \text{Li}}^\ominus - 2S_{298, \text{Ti}}^\ominus - 4 \cdot \frac{1}{2} S_{298, \text{O}_2}^\ominus$$

$$= (S_{298Li^+}^{\ominus} + 2S_{298Ti^{3.5+}}^{\ominus} + 4S_{298O^{2-}}^{\ominus}) - (S_{298Li}^{\ominus} + 2S_{298Ti}^{\ominus} + 4 \cdot \frac{1}{2} S_{298O_2}^{\ominus}) \quad (6)$$

Related values from the thermodynamics table can be utilized:

$$S_{298Li}^{\ominus} = 29.08 \text{ J} \cdot \text{mol}^{-1} \cdot \text{K}^{-1},$$

$$S_{298Ti}^{\ominus} = 30.760 \text{ J} \cdot \text{mol}^{-1} \cdot \text{K}^{-1},$$

$$\frac{1}{2} S_{298O_2}^{\ominus} = 102.57 \text{ J} \cdot \text{mol}^{-1} \cdot \text{K}^{-1}.$$

The above data are substituted into formula (6),

$$\Delta_f S_{298LiTi_2O_4}^{\ominus} = -312.03 \text{ J} \cdot \text{mol}^{-1} \cdot \text{K}^{-1}.$$

Therefore, the standard formation entropy of LiTi_2O_4 can be expressed as follows:

$$\Delta_f G_{298LiTi_2O_4}^{\ominus} = \Delta_f H_{298LiTi_2O_4}^{\ominus} - T \cdot \Delta_f S_{298LiTi_2O_4}^{\ominus} = (-2870648 + 312.03T) \text{ J} \cdot \text{mol}^{-1} \quad (7)$$

At last, the thermodynamic calculation of the carbon-thermal reduction reaction is carried out using Li_2CO_3 as the lithium source, TiO_2 as the titanium source, and starch as the carbon source. The reaction scheme can be expressed according to the following chemical reaction equation (8):



As for the unknown thermodynamic datum of Li_2CO_3 , TiO_2 and starch, the relational expression for $\Delta_f G^{\ominus}$ of eq. (8) and temperature T cannot be given. However, thermodynamic data of materials at a certain temperature can be inquired; therefore, we can calculate $\Delta_f G^{\ominus}$ at a certain temperature.

When T is 1073 K, it can be found that $\Delta G_{1073Li_2CO_3}^{\ominus} = -1390.56 \text{ KJ} \cdot \text{mol}^{-1}$, $\Delta G_{1073TiO_2}^{\ominus} = -1038.00 \text{ KJ} \cdot \text{mol}^{-1}$, $\Delta G_{1073C}^{\ominus} = -14.70 \text{ KJ} \cdot \text{mol}^{-1}$, and $\Delta_f G_{1073CO_2}^{\ominus} = -395.91 \text{ KJ} \cdot \text{mol}^{-1}$.

From formula (7), it is calculated that $\Delta_f G_{1073LiTi_2O_4}^{\ominus} = -2527.41 \text{ KJ} \cdot \text{mol}^{-1}$.

Therefore, $\Delta_f G_{1073K} = (4 \Delta_f G_{1073LiTi_2O_4}^{\ominus} + 3 \Delta_f G_{1073CO_2}^{\ominus}) - (2 \Delta G_{1073Li_2CO_3}^{\ominus} + 8 \Delta G_{1073TiO_2}^{\ominus} + \Delta G_{1073C}^{\ominus}) = [4 \times (-2527.41) + 3 \times (-395.91)] - [2 \times (-1390.56) + 8 \times (-1038.00) + (-14.70)] = -197.52 \text{ KJ} \cdot \text{mol}^{-1} < 0$.

Similarly, $\Delta_f G_{1123K} = -65.06 \text{ KJ} \cdot \text{mol}^{-1} < 0$, and $\Delta_f G_{1173K} = -32.53 \text{ KJ} \cdot \text{mol}^{-1} < 0$.

The standard Gibbs free energies of formation of LiTi_2O_4 at 1073 K, 1123 K and 1173 K are less than zero, which indicates that this carbon-thermal solid phase reaction can be performed when the temperature is more than 1073 K. Based on the calculation results of the thermodynamics, it was proven that the carbon-thermal reaction is feasible technology for fabricating LiTi_2O_4 material.

3.2 Material characterization

A typical SEM image of the as-prepared LiTi_2O_4 powders is shown in Fig. 1. The LiTi_2O_4 particles are almost sphere-like, and the average size of most particles is approximately 0.4-1.2 μm . It is observed that some spherical particles are agglomerated.

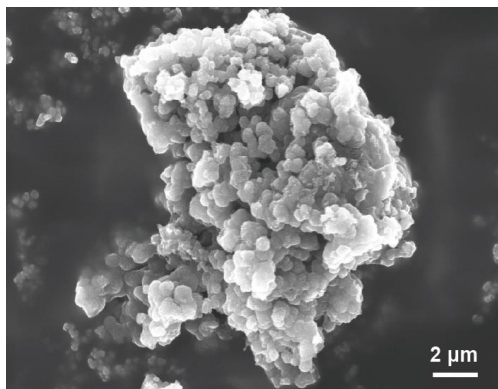


Figure 1. SEM image of LiTi_2O_4 prepared by the carbon-thermal reduction method.

The XRD pattern of the LiTi_2O_4 sample synthesized by carbon-thermal reduction is shown in Fig. 2. It can be ascertained that the mixture phases of LiTi_2O_4 and a tiny impurity phase of rutile- TiO_2 are both observed, and the dominant phase is LiTi_2O_4 . However, no carbon phase is detected in the XRD pattern. This is most likely due to the low content or amorphism for carbonized production. The peaks at 2θ angles of 18.4° , 35.6° , 43.3° , 57.2° , 62.8° , 65.8° and 79.3° correspond to the (111), (311), (400), (511), (440), (531) and (444) reflections of LiTi_2O_4 , respectively. All reflections observed in the data image have been indexed according to the $Fd3m$ space group of the cubic spinel structure with a unit-cell dimension of 8.340 \AA . The results are in good agreement with a previous X-ray diffraction report [19]. The sharp diffraction peaks indicate that the obtained LiTi_2O_4 is well crystallized.

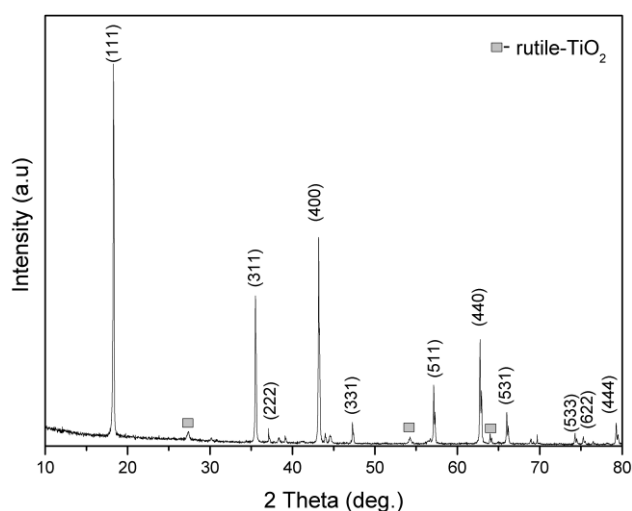


Figure 2. XRD pattern of LiTi_2O_4 prepared by the carbon-thermal reduction method.

3.3 Electrochemical properties

Fig. 3 shows multi-sweep cyclic voltammograms of LiTi_2O_4 prepared by the carbon-thermal reduction method. It is observed that the cyclic peak potentials of the symmetrical redox peaks

occurred at approximately 1.29 and 1.75 V, except the first sweep cyclic voltammetry, and the average potentials are approximately 1.52 V. For rutile-TiO₂, the peak potentials inserted and de-inserted by lithium ions are approximately 1.45 and 2.36 V, respectively [11]. Therefore, the first sweep cyclic voltammetry may be regarded as the joint effect of LiTi₂O₄ and rutile-TiO₂. Multi-sweep cyclic voltammetry curves are almost equivalent with only the appearance of a slight fading in the charge quantity of insertion and de-insertion, indicating that the reversibility of the LiTi₂O₄ active material is very good.

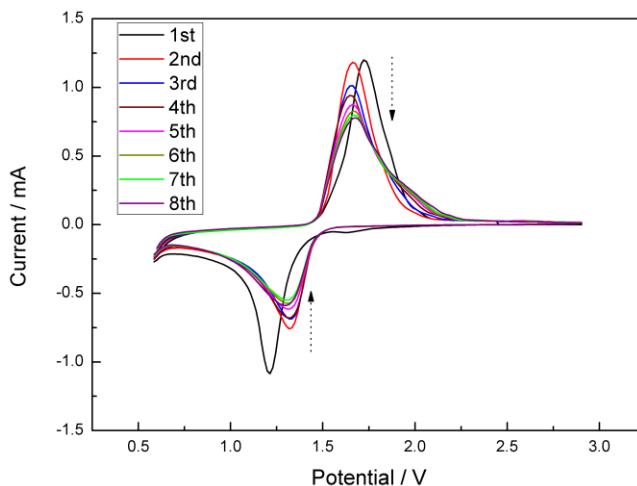


Figure 3. Multi-sweep cyclic voltammograms of the LiTi₂O₄ electrode in 1 M LiPF₆ / EC-DMC-DEC electrolyte, scan rate 0.5 mV·s⁻¹.

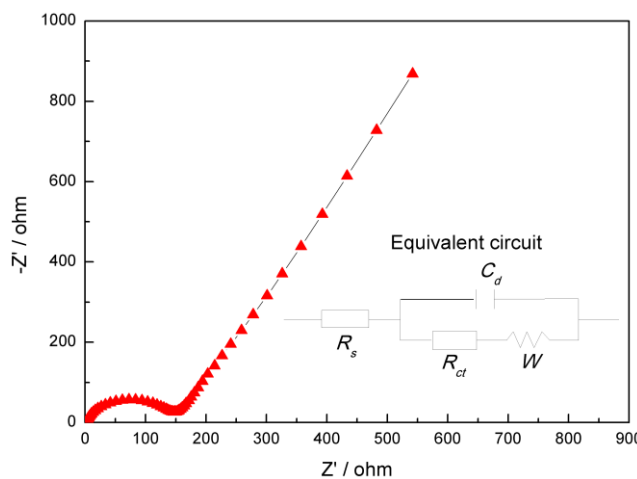


Figure 4. Nyquist plot of the LiTi₂O₄ at open-circuit state after discharge.

The surface reaction activity of the LiTi₂O₄ electrode material, such as charge transfer and lithium ion diffusion kinetics, is characterized by the electrochemical impedance spectroscopy (EIS), as shown in Fig. 4. The Nyquist plot is composed of a depressed semicircle in the medium-frequency region and a ~45° inclined straight line in the low-frequency region. The intercept impedance on the Z

real axis is regarded as the ohmic resistance, which is primarily related to the resistance of the electrolyte and electrode (R_s). It was observed that the ohmic resistance R_s is approximately 3.28Ω , which is lower than that for $\text{Li}_4\text{Ti}_5\text{O}_{12}$ [20]. The depressed semicircle in the middle-frequency region is attributed to the charge transfer resistance (R_{ct}) between the electrode active material and the liquid electrolyte, which corresponds to 148.50Ω . No semicircle is discovered in high frequency, indicating that the LiTi_2O_4 electrode does not have the diffusion resistance of lithium ions through the SEI layer [21]. At this point, the LiTi_2O_4 anode is much safer compared with lithium metal and carbonaceous anodes. The straight line in the low frequency is closely related to lithium ion diffusion in the LiTi_2O_4 electrode, corresponding to the Warburg impedance.

Charge/discharge curves in the second and tenth cycles of the LiTi_2O_4 electrode at a 0.2 C current rate are shown in Fig. 5. Extreme plateaus are observed, and a rather narrow gap between charge and discharge plateaus appeared, which indicates a high lithium ion extraction–insertion kinetics [22]. The discharge capacity in the second and tenth cycle of the LiTi_2O_4 electrode is 139.0 and 138.1 mAh/g, respectively, which is only slight fading. The average plateau potential is approximately 1.51 V, which is in accordance with the CV experimental results.

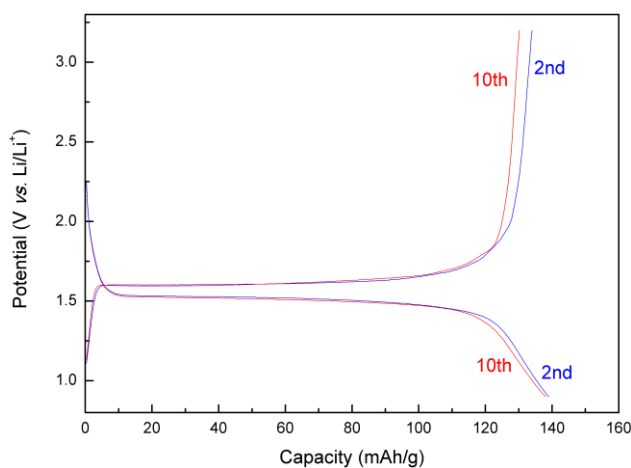


Figure 5. Discharge and charge curves of the LiTi_2O_4 electrode at a 0.2 C current rate.

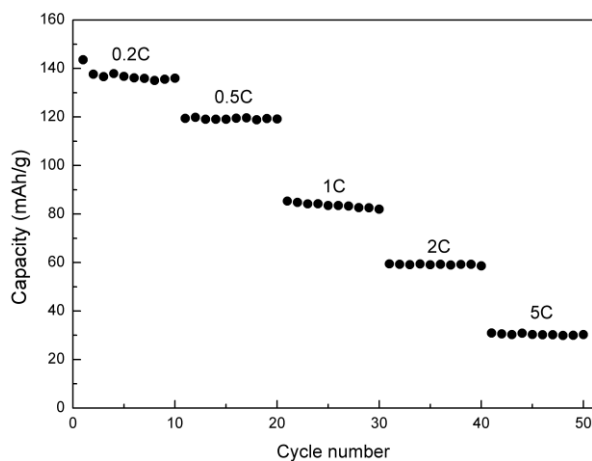


Figure 6. Cycling performance of the LiTi_2O_4 electrode at different C rates.

The plots of discharge retention versus cycle number at different C rates are shown in Fig. 6. A specific discharge capacity of the LiTi_2O_4 electrode after 10 cycles at 0.2C is 135.9 mAh/g. This value gradually decreases as the rates increases. When the current rate increases from 0.2 to 5C, the discharge capacity declines from 135.9 to 30.3 mAh/g after 50 cycles. Furthermore, it can be seen that the curves are relatively flat, which indicates that LiTi_2O_4 material has good cycling performance.

4. CONCLUSIONS

In this paper, we have successfully synthesized LiTi_2O_4 by a carbon-thermal reduction method. The thermodynamic calculation results indicate that the carbon-thermal reaction method is available. The XRD results show that LiTi_2O_4 has a spinel structure with space group $Fd3m$. The SEM image shows that the particle size of LiTi_2O_4 is approximately 0.4-1.2 μm . Symmetrical redox peaks at approximately 1.52 V versus Li/Li^+ , resulting from the insertion and extraction of lithium ion at LiTi_2O_4 , are observed in the cyclic voltammetry curve. Electrochemical measurements, including galvanostatic charge/discharge tests, specific capacity and cycling performance, show that the as-synthesized LiTi_2O_4 has excellent electrochemical performances.

ACKNOWLEDGEMENTS

The authors would like to acknowledge financial support from the National Natural Science Foundation of China (Grant No. 51604157), Project supported by the National Science Foundation for Post-doctoral Scientists of China (Grant No. 2016M591812), the Natural Science Foundation of Jiangsu Province, China (Grant No. BK20140870), and the Science Foundation of Nanjing University of Posts and Telecommunications: NUPTSF (Grant No. NY214045).

References

1. J. W. Choi and D. Aurbach, *Nat. Rev. Mater.*, 1 (2016) 16013.
2. X. Jia, Y. Lu, F. Wei, *Nano Research*, 9 (2016) 230.
3. L. Lu, X. Han, J. Li, J. Hua and M Ouyang, *J. power sources.*, 226 (2013) 272.
4. M. G.Verde, L.Baggetto, N. Balke, G. M.Veith, J. K.Seo, Z. Wang and Y. S. Meng, *ACS Nano*, 10 (2016) 4312.
5. J. F. Peters, M. Baumann, B. Zimmermann, J. Braun and M. Weil, *Renewable Sustainable Energy Rev.*, 67 (2017) 491.
6. J.-M. Tarascon and M. Armand, *Nature*, 414 (2001) 359.
7. L. Shen, E. Uchaker, X. Zhang and G. Cao, *Adv. Mater.*, 24 (2012) 6502.
8. X. Sun, P. V. Radovanovic and B. Cui, *New J. Chem.*, 39 (2015) 38.
9. E. Pohjalainen, T. Rauhala, M. Valkeapää, J. Kallioinen and T. Kallio, *J. Phys. Chem. C*, 119 (2015) 2277.
10. L. Yu, H. B. Wu and X. W. Lou, *Adv. Mater.*, 25 (2013) 2296.
11. J. Yang, J. Zhao, Y. Chen and Y. Li, *Ionics*, 16 (2010) 425.
12. A. Kitada, A. M. Arevalo-Lopez and P. Attfield, *Chem. Commun.*, 51 (2015) 11359.
13. D. C. Johnston, H. Prakash, W. H. Zachariasen and R. Viswanathan, *Mater. Res. Bull.*, 8 (1973) 777.
14. M. Pan, Y. Chen and H. Liu, *Ionics*, 21 (2015) 2417.
15. C. Feng, L. Li, Z. Guo, D. Shi, R. Zeng and X. Zhu, *J. Alloys Compd.*, 478 (2009) 767.
16. K. Jiang, X. Hu, H. Sun, D. Wang, X. Jin, Y. Ren and G. Z. Chen, *Chem. Mater.*, 16 (2004) 4324.

17. A. Kumatani, T. Ohsawa, R. Shimizu, Y. Takagi, S. Shiraki and T. Hitosugi, *Appl. Phys. Lett.*, 101 (2012) 123103.
18. K. Jin, G. He, X. Zhang, S. Maruyama, S. Yasui, R. Suchoski, J. Shin, Y. Jiang, H. Yu and J. Yuan, *Nat. Commun.*, 6 (2015) 7183.
19. W. Y. Ra, M. Nakayama, Y. Uchimoto, and M. Wakihara, *J. Phys. Chem. B*, 109 (2015) 1130.
20. Z. Yu , G. Zhu, H. Xu and A. Yu, *Energy Technol.*, 2 (2014) 767.
21. J. Liu, W. Liu, S. Ji, Y. Wan, H. Yin and Y. Zhou, *Eur. J. Inorg. Chem.*, 12 (2014) 2073.
22. J. Ni, L. Yang, H. Wang and L. Gao, *J. Solid State Electrochem.*, 16 (2012) 2791.

© 2018 The Authors. Published by ESG (www.electrochemsci.org). This article is an open access article distributed under the terms and conditions of the Creative Commons Attribution license (<http://creativecommons.org/licenses/by/4.0/>).